Lasers in Manufacturing Conference 2023

Anamorphic beam shaping for glass nanofibers production by continuous fiberizing by laser melting (Cofiblas)

Joaquín Penide[a], Félix Quintero[a,b,*], José Luis Fernández[b], Mónica Fernández-Arias[a,b], Raúl Barciela[a,b], Jesús del Val[c], Fernando Lusquiños[a,b], Juan Pou[a,b]

[a]*CINTECX, Universidade de Vigo, LaserON research group, 36310 Vigo, España.*
[b]*Applied Physics Department, Universidade de Vigo, E.E.I., 36310 Vigo, España.*
[c]*Centro Universitario de la Defensa, Escuela Naval Militar, Plaza de España 2, 36920 Marín, España.*

Abstract

The use of glass nanofibers as reinforcements in composite materials promises a substantial enhancement of their performance thanks to their superior mechanical properties. The continuous fiberizing by laser melting (Cofiblas), makes possible to obtain ultrafine fibers with virtually infinite length and capability to feasibly scaling up for mass production. The effectiveness of this technique relies on several factors, being the laser beam shaping system the more relevant one. In this work we compare two different optical systems: one constituted by spherical lenses, and the second one based on an anamorphic system which generates an elliptical Gaussian distribution of the laser beam irradiance. Both configurations are evaluated in several sets of experiments with the main target of obtaining continuous glass nanofibers with the smallest diameter. As a result, continuous silica nanofibers with diameters 84.5% smaller are obtained with the anamorphic system thanks to the increase of energy absorbed by the filament.

Keywords: anamorphic optics; laser beam shaping; glass nanofibers; laser glass processing; Cofiblas

1. Introduction

In the search for better mechanical features and lightweight materials, nanofibers and nanowires have been pointed out as reinforcement for potentially high-performance composites (Ritchie, 2011). This is because strength and toughness of fibers increase significantly for decreasing diameters (Griffith and Taylor, 1921) (Peng, Nain and Mirzaeifar, 2019). Nanofiber reinforced composites have shown an improvement in

* Corresponding author. *E-mail address: fquintero@uvigo.es*

their mechanical behavior, nevertheless, the use of short discontinuous fibers or the inadequate alignment of this reinforcements could mean that those mechanical properties do not improve as much as expected (Dzenis, 2008).

Glass fibers occupy a prominent place in the fiber-reinforced composites market, where their good mechanical properties and optimal photochemical durability at affordable costs are required in applications such as aerospace, automotive and wind turbine manufacturing (Erden and Ho, 2017). The sustainable mass production of glass nanofibers augurs a substantial enhancement of their applications thanks to a substantial enhancement of their mechanical properties. The industrial production of glass fibers is routinely made by melt spinning. A technique which involves melting an enormous volume of glass and subsequent stretching of a molten filament by mechanically drawing it to a reel from the bushing tip or from the molten preform. However, conventional melt spinning processes are not able to produce fibers thinner than about 2 µm (Wallenberger and Bingham, 2010).

Continuous fiberizing by laser melting and supersonic dragging (Cofiblas) is a novel technique recently developed by the authors to produce glass nanofibers with exceptional small diameter and virtually unlimited length (Quintero *et al.*, 2020). In addition, the diameter of the obtained fibers can be precisely controlled, producing nonporous, solid and free-standing separated nanofibers. This unprecedented process combines a high-power laser with a supersonic gas jet to reduce the diameter of a glass preform. Figure 1 presents an scheme of the experimental set-up to run the Cofiblas process. Specifically, it employs a high power CO_2 laser and a beam-splitter that divides the continuous emission into two identical laser beams. Both laser beams are redirected by several mirrors through the Beam Shaping System (BSS) and oriented so as they face each other on the precursor material.

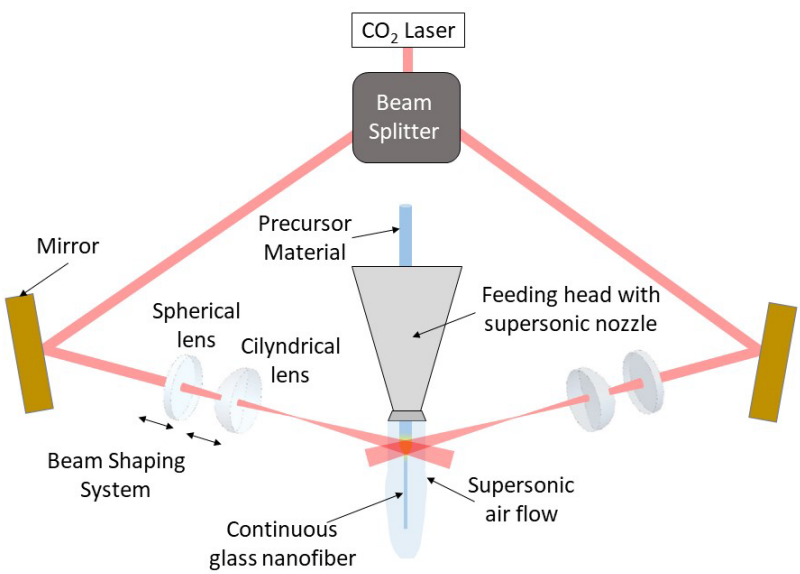

Fig. 1. Schematic representation of the experimental set-up for the Cofiblas technique. It shows in red the laser beam emerging from the CO_2 laser which is divided into two beams, each of them with half the total power, by the beam splitter. Both laser beams and directed to the glass preform using copper mirrors and the irradiance distribution is adjusted using the Beam Shaping System (BSS). The glass preform is continuously feed coaxially with the supersonic air jet which stretches the molten preform.

The most important achievements of this technique are the quick heating, stretching and cooling of the preform, which all together lead to the high stability in continuous operation, which in turn makes possible that these fibers are virtually endless. The high energy delivered by the laser leads to extreme temperature gradients, thus the Cofiblas process is able to elongate the preform at extremely high strain rates, reducing its diameter from several tenths of millimeter into a nanofiber in some milliseconds. The supersonic gas jet produces a distributed stretching force around and along the molten material. The axial distribution of the elongational forces is essential for the stability of the process, since it allows to reach a large axial stress and strain ratios at the sections where the filament is molten, and, conversely, very low stress where the nanofiber is solid and can't withstand the high tensile force required to stretch the molten filament (Quintero *et al.*, 2020).

A precise heating and cooling of the filament is also crucial. The use of two laser beams guarantees an uniform distribution of the energy on the preform. Also, a precise control of the irradiance along the stretching zone is required to keep the stability of the molten filament. The glass preform must be heated to a temperature range corresponding to a suitable viscosity window for the elongation process, called the fiber forming viscosity (Wallenberger and Bingham, 2010) (Quintero *et al.*, 2014). A high irradiance peak could lead to excessive filament temperature and the viscosity drops below the lower limit, which disturbs the stability of the process and causes the fiber breakage. On the contrary, a reduced irradiance leads to a low temperature, exceeding the upper viscosity limit, and, consequently, the tensile force exerted by the gas flow is not able to stretch the molten material, resulting in a thick fiber. Additionally, the irradiance profile must be adapted to the reduction of diameter of the filament, since the energy absorbed by the preform at the beginning of the process is high enough to initiate its elongation with moderately high irradiance. However, as the diameter of the filament decreases, so does the absorbed energy, just because the irradiated volume is getting smaller. Consequently, a precise control of the irradiance distribution along the filament is required. For this reason, the adequate design of the BSS is crucial for the proper functioning of the process, since it allows to obtain an adequate distribution of irradiance along the axis of the filament and a precise control thereof. The present paper, presents the set-up of the BSS employed to adjust the irradiance profile on the filament in the Cofiblas technique, designed to increase the stability of the process and give a continuous nanofiber.

2. Materials and methods

A high-power CO_2 laser (Rofin DC-035) was employed. This laser source gives a maximum output radiant power of 3.5 kW with a beam transverse mode very close to TEM00 ($M^2 \leq 1.05$). It was operated in continuous regime and wavelength λ=10.6 μm. The optical system, includes a beam splitter together with two symmetric mirrors and two Beam Shaping Systems (BSS), see Figure 1. First, the laser beam is divided into two by means of the beam splitter 50/50 (Rofin EBS). The beam splitter includes a diamond window which reflects 50 % of the beam with the same original beam profile, the remaining 50 % pass through the diamond window with an accuracy of < 1 % between both laser beams. Each beam is redirected by a plane copper mirror to hit the preform at the outlet of the nozzle. The BSS is adjusted to accurately distribute the radiant power of each beam along the *x* and *y* axis (see Fig. 2), in order to obtain the proper irradiance distribution.

Pure silica fibers (CeramOptec, Germany) with 600 μm of diameter were employed as the precursor material in all experiments. The process gas employed was compressed air supplied at a pressure of 350 kPa to the de Laval nozzle, which generates a supersonic gas jet to stretch the molten filament. The morphology of the fibers was characterized using a field-emission SEM (JEOL JSM-6700F), as-produced fibers were deposited on carbon adhesive discs for SEM imaging and their diameters were measured in the calibrated

micrographs. A minimum of five fibers were measured in a single experiment, but the typical number of samples was around fifteen.

2.1. Design and calculations of the BSS-2 with cylindrical and spherical lenses

The beam shaping system based on an anamorphic optical system was designed with the purpose of optimizing the irradiance distribution of the laser beam along the filament axis (*y*-axis in Fig. 2). Different anamorphic configurations comprising lenses, mirrors, and/or prims are available for different purposes (Zhang *et al.*, 2019; Kumstel, 2021). In our case, the goal of the anamorphic system is simply to reshape and focus a collimated high-power laser beam, so a combination of a spherical lens with a cylindrical lens was chosen because this configuration provides appropriate beam quality while maintaining simplicity, a small number of optical surfaces, ruggedness and low cost.

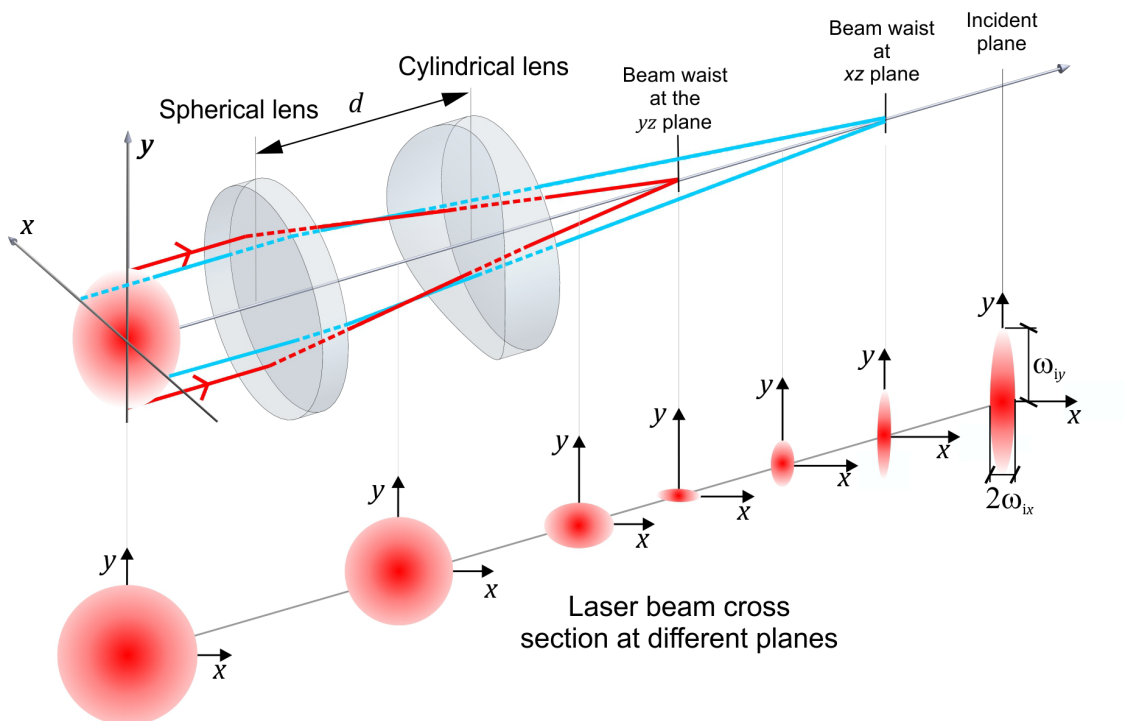

Fig. 2. Representation of the BSS that we designed together with a representation of the Gaussian beam propagation. First, a plano-convex spherical lens ($f_s = 710$ mm) is situated at the distance previously calculated from the incident plane on the glass preform. Then, the plano-convex cylindrical lens with focal length $f_c = 267$ mm is situated at the distance *d* from the spherical lens, with its rotation axis parallel to the *x*-axis. The input beam of the BSS is the collimated beam emitted by the laser (once divided in two by means of the beam splitter) entering the spherical lens.

An analytical calculation of the Gaussian beam propagation through the optical system for different combinations of spherical and cylindrical lenses (either convergent or divergent) was carried out to select the proper lens combination (Penide *et al.*, 2022). In this analysis, we assume that the cylindrical lens transforms

the original circular Gaussian beam into an elliptic Gaussian beam (Yariv, 1989) which exhibits simple (or orthogonal) astigmatism: the light spot is elliptical with the same orientation in every beam cross section, so there are two principal meridional planes, perpendicular to each other, which contain the propagation axis of the beam and the major or minor axis of the ellipses of constant irradiance. The irradiance profile varies as the beam propagates through space, and can be expressed in a Cartesian coordinate system as:

$$I\,(x,y,z) = I_0\,\frac{\omega_{0x}\omega_{0y}}{\omega_x(z)\omega_y(z)}\exp\left[-2\left(\frac{(x-x_c)^2}{{\omega_x}^2(z)}+\frac{(y-y_c)^2}{{\omega_y}^2(z)}\right)\right] = I_0(z)\exp\left[-2\left(\frac{(x-x_c)^2}{{\omega_x}^2(z)}+\frac{(y-y_c)^2}{{\omega_y}^2(z)}\right)\right] \quad (1)$$

where the *z*-axis is parallel to the direction of propagation, I_0 is a constant, $I_0(z)$ is the irradiance at the center of the beam cross section at an arbitrary *z* position, $x - x_c$ and $y - y_c$ are the distances from the propagation axis of the beam on the principal meridional planes, $\omega_x(z)$ and $\omega_y(z)$ are the respective Gaussian beam radii, where the irradiance is $1/e^2$ (13.5 %) of $I_0(z)$, and ω_{0x} and ω_{0y} are the Gaussian beam radii at the respective waists, which occur at different *z* values. If we choose the *z* axis to coincide with the propagation axis of the beam, then $x_c = y_c = 0$. The value of $I_0(z)$ can be related to the total radiant flux (or radiant power) of the laser beam, Φ_e, by integrating the irradiance over the cross section:

$$\Phi_{\mathrm{e}} = \iint_{-\infty}^{\infty} I_0(z)\exp\left[-2\left(\frac{(x-x_c)^2}{{\omega_x}^2(z)}+\frac{(y-y_c)^2}{{\omega_y}^2(z)}\right)\right]dx\,dy = (1/2)I_0(z)\,\pi\,\omega_x(z)\,\omega_y(z) = (1/2)I_0\,\pi\,\omega_{0x}\,\omega_{0y} \quad (2)$$

Using the procedure explained in our previous work, we calculate the positions of the lenses that give an irradiance distribution in the plane of incidence characterized by the lengths of the semi-axes corresponding to the elliptical Gaussian beam, as shown in Fig. 2. In this representation, ω_{ix} and ω_{iy} are the respective semi-axes length of the elliptical cross section of the laser beam.

2.2. Design of experiments.

Due to the wide number of factors involved, we used the design of experiments (DoE) methodology in order to analyze the influence of the optical configurations on the characteristics of the fibers obtained. The experiments were carried out using a total factorial design, which means that all possible combinations of factors and levels were obtained. Two different full factorial DoEs, each one with three factors in two levels were planned. The first two factors: length of the major axis ($2\omega_{iy}$) and area of the elliptical cross section (A) of the laser beam are parameters related to the irradiance distribution of the laser beam on the filament. The third factor, *v*, is the feeding speed of the preform to the nozzle, which gives the axial velocity of the filament at the beginning of the elongation. In all experiments, the major axis of the elliptical laser beam cross section corresponds to the principal meridional plane aligned with the filament axis, and the total radiant power of the laser beam, Φ_e, is independently adjusted at each trial, progressively increasing it up to the maximum value which yields continuous fibers without filament breaking. Factors with the corresponding levels used in the first DoE1 are detailed in Table 1.

Table 1. DoE1

Factors	Level 1	Level 2
Major axis ($2\omega_{iy}$ / mm)	30	45
Spot area (A / $\pi \cdot 4^{-1}$ mm^2)	90	180
Feeding speed (v / μm·s^{-1})	100	500

A second set of experiments was carried out with a significant reduction of the feeding rate (DoE2). In this case, a preliminary set of tests was performed in order to determine the most suitable conditions, which brought to light that the smallest diameters are obtained in the case of the shorter major axis of the laser beam. In addition, there is a tendency to decrease the diameter as the feeding speed decreases. In view of these results, a range of smaller major axes than those used in DoE1 were chosen. Table 2 shows the factors and levels of DoE2.

Table 2. DoE2

Factors	Level 1	Level 2
Major axis ($2\omega_{iy}$ / mm)	20	30
Spot area (A / $\pi \cdot 4^{-1}$ mm^2)	40	60
Feeding speed (v / μm·s^{-1})	1	4

3. Results and discussion

Table 3 details the processing conditions and resulting mean diameters for each test carried out within the framework of DoE1, including only those that ensure to obtain continuous fibers. The fibers generated have a smooth cylindrical shape with uniform diameter along their entire length. The analysis reveals the notable effect of the major axis of the elliptical laser beam, $2\omega_{iy}$, in this region of values of the factors studied. In particular, there is a tendency to decrease the diameter as ω_{iy} increases. The same is also observed for the feeding speed, but in this case the trend is less pronounced. Regarding the area of the laser beam at the working point, the tendency is to decrease the diameters as the area increases. This indicates that to optimize results, the differences between the irradiance applied when starting to stretch the preform and the peak irradiance should not be too pronounced, but the distance should be relatively high. The diameters of the fibers produced are still high. The reason for this result is that this range of feeding speed was found to be too high, in relation to the maximum radiant flux available with the current laser equipment, notice that the maximum radiant power attainable by this laser (1750 W for each beam) was employed in some trials. Then, the maximum temperature reached in the filament is limited by the laser power, consequently it can't reach the lower level of viscosity in the working window required to quickly elongate the preform down to the nanometric diameter. The minimum mean diameters obtained fell slightly below 9 μm, while the maximum diameters are close to 40 μm.

Table 3. Processing conditions with the corresponding mean diameters obtained by the set of operating parameters of DoE1. Φ_e is the radiant flux of each laser beam, *v* is the feed speed, $2\omega_{iy} \times 2\omega_{ix}$ is the length of the major axis times the minor axis incident plane of the preform, being A its area. D_m is the mean diameter of the resulting fibers and σ its standard deviation.

v / µm·s^{-1}	*A* / (π·4^{-1} mm^2)	$2\omega_{iy} \times 2\omega_{ix}$ / mm^2	Φ_e / W	D_m / µm	σ / µm
100	90	30 × 3	210	34.04	4.38
100	90	45 × 2	1750	7.62	0.58
100	180	30 × 6	1000	14.69	1.38
100	180	45 × 4	1750	15.62	2.64
500	90	30 × 3	263	19.22	6.02
500	90	45 × 2	560	8.83	4.76
500	180	30 × 6	370	21.98	2.38
500	180	45 × 4	1750	8.93	1.94

In the second set of the factorial experiments, DoE2, a much lower range of feeding speeds was employed. The processing conditions and the resulting mean diameters for each test are detailed in Table 4. Again, the results reveal a significant influence of the major axis of the elliptical laser beam, $2\omega_{iy}$, and its area on the diameter of the fibers. Both effects are related with the length of the segment of material irradiated and the progressive change of irradiance along it, in the same way as explained in the previous paragraphs. As the major axis of the cross section is increased the laser beam reaches a longer segment of the preform with a proper level of irradiance, the filament keeps the suitable viscosity for stretching along a longer length and, consequently, the elongation continues down to a lower diameter. On the contrary, an increase in speed has the opposite effect. The best results were obtained with high radiant power (1750 W) and low feeding speed (1 µm/s), leading to obtain fibers with the smallest mean diameter (0.37µm). The diameters obtained in this set of experiments are one order of magnitude smaller than those obtained previously in DoE1, which reflects the enormous influence of the speed.

Therefore, results of the set of experiments DoE1 and DoE2 led to the same trends even though they produce fibers of different diameters. On one hand, by decreasing the feeding speed, the fibers produced have smaller diameters. On the other hand, by increasing the length of the segment irradiated by the laser beam with a higher irradiance level, also implies an improvement of the diameters. These results, bring to light the improvement that involves the implementation of the simple anamorphic beam-shaping system based on the combination of spherical and cylindrical lenses to obtain a suitable irradiance distribution. This combination allowed to increase the irradiance along the axis in the direction of the preform (*y*-axis / major axis), while the width of the laser beam at the incident plane (*x*-axis / minor axis) can be reduced independently to adjust it to the filament diameter. This distribution provides a high level of irradiance at the point where the filament begins to stretch and, at the same time, the maximum is reached at a distance sufficiently far from the start to coincide with a notable reduction in the diameter of the filament. In this way, the elongation of the filament is extended until the diameter and irradiance are already markedly reduced, what makes it possible to obtain finer fibers. This effect was observed experimentally and analysed using mathematical modelling in our previous publication (Quintero *et al.*, 2020).

Table 4. Processing conditions with the corresponding mean diameters obtained by using the BSS-2 in DoE2. Φ_e is the radiant flux of each laser beam, *v* is the feed speed, $2\omega_{iy} \times 2\omega_{ix}$ is the length of the major axis times the minor axis incident plane of the preform, being A its area. D_m is the mean diameter of the resulting fibers and σ its standard deviation.

v / µm·s^{-1}	*A* / (π·4^{-1} mm^2)	$2\omega_{iy} \times 2\omega_{ix}$ / mm^2	Φ_e / W	D_m / µm	σ / µm
1	40	20 × 2	275	2.05	0.64
1	60	20 × 3	450	1.40	0.52
1	40	30 × 1.3	1,750	0.62	0.17
1	60	30 × 2	1,750	0.37	0.08
4	40	20 × 2	225	5.68	2.05
4	60	20 × 3	400	1.91	0.44
4	40	30 × 1.3	1,750	1.00	0.47
4	60	30 × 2	1,750	0.49	0.1

4. Conclusions

In this contribution, a simple design of an anamorphic beam forming system is presented to convert the circular Gaussian beam profile of a high power CO_2 laser into an elliptical Gaussian profile with orthogonal astigmatism. The design of the lens system and its arrangement is obtained by means of the Gaussian beam propagation equations that allow calculating the irradiance distribution in the two main beams. The efficacy and usefulness of this beam-shaping system was demonstrated experimentally through an extensive series of glass nanofiber production experiments using the Cofiblas technique.

Acknowledgements

We acknowledge the help of A. Abalde with the construction of the experimental system. Technical staff of CACTI at University of Vigo is also acknowledged by their help with the characterization of some samples.

Funding: This work was partially supported by the EU research project Bluehuman (EAPA_151/2016 Interreg Atlantic Area), Government of Spain [PID2020-117900RB-I00 (MCI/AEI/FEDER, UE), FPU20/03112, Margarita Salas Postdoc Fellowship Program, M. Fernández Arias], and by Xunta de Galicia (ED431C 2019/23).

References

Dzenis, Y. (2008) 'Structural nanocomposites', *Science*, 319(5862), pp. 419–420. doi: 10.1126/science.1151434.

Erden, S. and Ho, K. (2017) '3 - Fiber reinforced composites', in Seydibeyoğlu, M. Ö., Mohanty, A. K., and Misra, M. (eds) *Fiber Technology for Fiber-Reinforced Composites*. Woodhead Publishing (Woodhead Publishing Series in Composites Science and Engineering), pp. 51–79. doi: https://doi.org/10.1016/B978-0-08-101871-2.00003-5.

Griffith, A. A. and Taylor, G. I. (1921) 'The phenomena of rupture and flow in solids', *Philosophical Transactions of the Royal Society of London. Series A, Containing Papers of a Mathematical or Physical Character*. Royal Society, 221(582–593), pp. 163–198. doi: 10.1098/rsta.1921.0006.

Kumstel, J. (2021) 'Laser polishing of metallic freeform surfaces by using a dynamic laser beam preforming system', *Journal of Laser Applications*. Laser Institute of America, 33(2), p. 22020. doi: 10.2351/1.5128459.

Peng, K., Nain, A. and Mirzaeifar, R. (2019) 'Tracking the origins of size dependency in the mechanical properties of polymeric nanofibers at the atomistic scale', *Polymer*. Elsevier, 175(December 2018), pp. 118–128. doi: 10.1016/j.polymer.2019.05.014.

Penide, J. *et al.* (2022) 'Anamorphic beam shaping system designed to optimize irradiance distribution in the Cofiblas process for glass nanofibers production', *Optics and Lasers in Engineering*, 152(January), p. 106972. doi: 10.1016/j.optlaseng.2022.106972.

Quintero, F. *et al.* (2014) 'Nonconventional production of glass nanofibers by laser spinning', *Journal of the American Ceramic Society*, 97(10), pp. 3116–3121. doi: 10.1111/jace.13127.

Quintero, F. *et al.* (2020) 'Continuous fiberizing by laser melting (Cofiblas): Production of highly flexible glass nanofibers with effectively unlimited length', *Science Advances*. American Association for the Advancement of Science, 6(6), p. eaax7210. doi: 10.1126/sciadv.aax7210.

Ritchie, R. O. (2011) 'The conflicts between strength and toughness', *Nature Materials*. Nature Publishing Group, 10(11), pp. 817–822. doi: 10.1038/nmat3115.

Wallenberger, F. T. and Bingham, P. A. (2010) *Fiberglass and glass technology: energy-friendly compositions and applications*. Springer. doi: 10.1007/978-1-4419-0736-3.

Yariv, A. (1989) *Quantum Electronics*. 3rd edn, *John Wiley & Sons*. 3rd edn. New York.

Zhang, J. *et al.* (2019) 'Paraxial lens design of anamorphic lenses with a fixed anamorphic ratio', *OSA Continuum*. OSA, 2(4), pp. 1430–1454. doi: 10.1364/OSAC.2.001430.